Status of free-energy representations for the homogeneous electron gas

Valentin V. Karasiev,[1,*] S. B. Trickey,[2] and James W. Dufty[3]
[1]*Laboratory for Laser Energetics, Univ. of Rochester, 250 East River Road, Rochester, New York 14623, USA*
[2]*Quantum Theory Project, Dept. of Physics and Dept. of Chemistry, Univ. of Florida, Gainesville, Florida 32611-8435, USA*
[3]*Dept. of Physics, Univ. of Florida, Gainesville, Florida 32611-8435, USA*

(Received 1 February 2019; published 20 May 2019)

Renewed interest in the homogeneous electron gas (HEG) has been stimulated by recent accurate simulations of it over a wide range of densities and temperatures. Those data, combined with known theoretical limits, have led to analytical representations of the free energy. Such a representation is, at least in principle, the complete HEG equation of state. The initial objective here is to establish that the two best representations ["corrKSDT," Phys. Rev. Lett. **112**, 076403 (2014), Phys. Rev. Lett. **120**, 076401 (2018), and "GDB" Phys. Rev. Lett. **119**, 135001 (2017)] of the simulation data and constraints are effectively the same in both functional form and accuracy of representation. The second objective is to disclose and delineate a significant difficulty. Despite their expected accuracy for the free energy, the underlying functional form is not adequate for derived thermodynamic properties. As an example, the specific heats obtained from the representations exhibit anomalies suggesting the need first for additional simulation data in critical regimes, then for refined fitting functions. The existing representations are, however, almost certainly adequate for applications based on the free energy alone (e.g., density-functional theory for warm dense matter). The third objective is to show that, despite their inability to provide a complete thermodynamic description of the HEG, the best analytical representations do provide a fully adequate exchange-correlation local density approximation for free-energy density-functional calculations.

DOI: 10.1103/PhysRevB.99.195134

I. INTRODUCTION

The homogeneous electron gas (HEG) is a well-studied system at zero temperature as a model for electrons in solids, and as a model for fully ionized plasmas at temperatures T well above the Fermi temperature T_F. At intermediate temperatures and densities, for a long while far less information was available from either theory or simulation, in large part due to lack of motivation. That has changed recently with growing experimental access to observations on states of matter in this domain. Such access is driving growth in the fields of warm dense matter (WDM) and high energy density physics (HEDP). Accordingly, the first quantum Monte Carlo (QMC) simulations for the HEG in this domain were reported only six years ago [1]. Subsequently Dornheim *et al.* [2] produced improved QMC results for temperatures $0.5 \leqslant t = T/T_F \leqslant 8$ over a wide density range (Wigner–Seitz radii $0.1 \leqslant r_s \leqslant 10$). They also developed and used significantly improved finite-size corrections. Those data currently seem to be the most accurate finite-T HEG results available.

For practical purposes a representation interpolating such QMC data and extrapolating it via known theoretical limits is needed. The target is an equation of state for the complete thermodynamics of the HEG, provided by the free energy as a function of r_s and t. A rather complete review of the recent simulations and their representations is given in Ref. [3]. As noted there, the program for constructing the free energy from theoretical limits and simulation data originally was presented and used in Ref. [4]. That reference presented a representation, "KSDT," based on the original data of Ref. [1] and the $T = 0$ data of Ref. [5]. Subsequently Groth *et al.* [6] used the KSDT approach and protocol to reparametrize the exchange-correlation (XC) contribution to the free energy against the finite-size-corrected QMC results of Ref. [2] along with the Singwi–Tosi–Land–Sjölander (STLS) approximation [7] for low-t ($t < 0.5$) behavior and for connection with the $T = 0$ data of Ref. [5]. The resulting representation is denoted "GDB" (as in Ref. [3]). Essentially simultaneously, a small error in the use of zero-temperature data for KSDT was detected and repaired to yield the corrected KSDT representation "corrKSDT" (see Supplemental Material for Ref. [8]).

That is the context. The objectives here are threefold. First is to show that the representations, corrKSDT and GDB, give essentially indistinguishable free energies over the entire r_s, t plane of interest. That statement is only very slightly modified for KSDT compared with GDB. An even stronger equivalence of corrKSDT and GDB is observed for the XC contribution alone to the free energy.

The second objective is to point out that those two interchangeable representations do not seem to give accurate descriptions of *derived* HEG thermodynamic properties and to discuss the implications. Specifically, the T dependence reflected in the specific heat exhibits anomalies. Other possible peculiarities are associated with the extreme low-T specific heat (an effective-mass enhancement) and odd oscillations in the difference between fully polarized and unpolarized exchange free energies. We conclude that the present representations are incomplete for a full understanding and prediction of HEG thermodynamics. Consideration of the KSDT protocol

*vkarasev@lle.rochester.edu

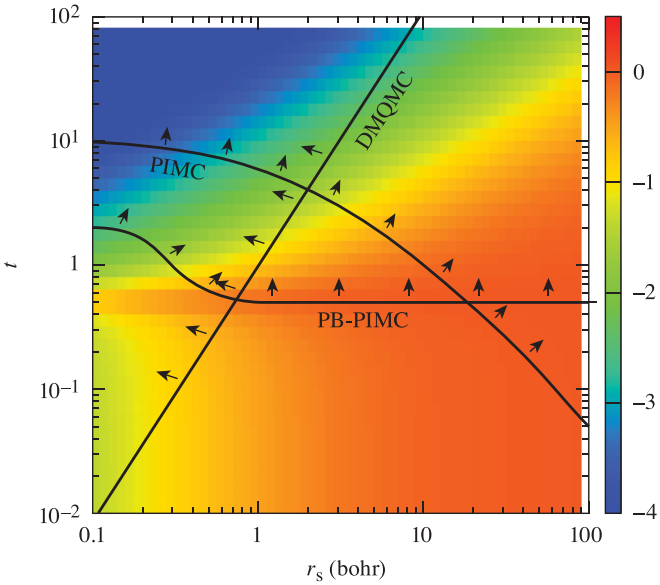

FIG. 1. The lower bound of relative magnitude of f_{xc} with respect to the total free-energy per particle, f_{tot}, for the HEG calculated as $\log_{10}(|f_{xc}(r_s,t)|/[|f_s(r_s,t)|+|f_{xc}(r_s,t)|])$. The denominator is defined as the sum of absolute values of two free-energy components to avoid meaningless values at conditions for which cancellation between f_s and f_{xc} occurs. Validity domains for PIMC, PB-PIMC, and DMQMC are in the directions away from the three curves indicated by the arrows. See text for notation.

that the representations share leads to some specific conclusions. Without additional, very accurate QMC data (and/or new formal constraints) for $t \leqslant 0.5$ and small r_s as well as dense sampling of the large-r_s ($r_s > 8$) region, a parametrization that gives accurate HEG temperature derivatives over a larger r_s, t domain seems unachievable.

Figure 1 illustrates the point. It shows the ratio of the XC free energy per particle, f_{xc}, to the upper bound of the total free energy per particle, $|f_s(r_s,t)|+|f_{xc}(r_s,t)|$, where f_s is the noninteracting free energy per particle as a function of r_s and t. Superimposed are three curves that delineate the parameter combinations (from Ref. [9]: the PIMC and PB-PIMC curves are extrapolated to the large-r_s values and the DMQMC curve is extrapolated to the high-T and low-T limits) for which three methods, standard path integral Monte-Carlo (PIMC), permutation-blocking PIMC (PB-PIMC) [10] and density-matrix QMC (DMQMC) [11], can be used to obtain accurate finite-T reference data for the HEG. The arrows with each curve point to the valid region. Evidently, the domain in which none of the accurate methods is applicable coincides with much of the region in which the XC free energy per particle has the same order of magnitude as the upper bound of the total free-energy per particle.

The third objective is to demonstrate that, despite those notable limitations of the current best representations of the HEG XC free energy, the most important application of those representations is unscathed. Specifically, those representations provide a thoroughly adequate local density approximation (LDA) to the XC free energy for density-functional theory (DFT) for calculation of properties for real systems of electrons and ions under the extreme conditions of WDM. We confirm that, for use as the LDA, corrKSDT and GDB are interchangeable and KSDT itself is essentially as good. Not only is this important in its own right, it is also critical for more sophisticated XC free-energy approximations based on exact limits and constraints. They must have the HEG as a limit. An example is the first finite-T generalized gradient approximation (GGA) XC free-energy functional [8]. It uses corrKSDT as its LDA ingredient, hence its HEG limit.

II. EQUIVALENCE OF REPRESENTATIONS

There are many representations for the HEG free energy based on approximate theories and various simulations (see Ref. [3] for a thorough description). Here and below, attention is primarily on corrKSDT and GDB as the most controlled and accurate incorporation of the latest QMC and theoretical constraints. KSDT enters because, as mentioned already and discussed where germane below, it differs only slightly from corrKSDT.

The universal part (i.e., that which is independent of any external potential) of the free energy per particle of a many-electron system conventionally is decomposed as a contribution from the noninteracting system, f_s, the Hartree contribution, f_H, and that from XC, f_{xc}:

$$f = f_s + f_H + f_{xc}. \tag{1}$$

For the HEG, f_s is a function of r_s and t which is known exactly and $f_H = 0$ because of the neutralizing background. Thus the difficult many-body challenge is determination of f_{xc}. Note that only the total free energy matters for observable physical quantities.

In this section, it is shown that the corrKSDT, KSDT, and GDB representations are all equivalent with respect to the total free energy $f(r_s,t)$ per particle. The stronger requirement of equivalence for $f_{xc}(r_s,t)$ also holds for corrKSDT and GDB. The former equivalence is important for DFT applications to, e.g., WDM; see below. The latter is of more consequence for understanding the origin of many-body XC effects in the HEG. Those are discussed in the next section.

Consider first the accuracy of KSDT as a representation of the best QMC data from Ref. [2]. Figure 2 shows the comparison of $f(r_s,t)$ as a function of t for several values of r_s. The agreement clearly is excellent. Quantitatively, the relative differences

$$\frac{\Delta f_{tot}}{|f_{tot}|} := \frac{\left|f_{tot}^{fit} - f_{tot}^{QMC}\right|}{|f_{tot}|} \tag{2}$$

for $t = 2$, 4, and 8 are 0.22% or below. For $t = 1$ the maximum relative difference is 0.35%. For $t = 0.5$ the relative difference has similar values for all r_s except $r_s = 0.5$, 0.4 and 0.3. At those values there is a cancellation between the f_s and f_{xc} terms, the denominator in Eq. (2) thus becomes small, and the relative difference increases to 0.87%, 1.14%, and 6.89%, respectively.

What is not evident from Fig. 2 is the fact that $|f_s(r_s,t)| \gg |f_{xc}(r_s,t)|$ for the domain of high density, $r_s < 1$, and comparatively high temperature, $t \geqslant 2$. Regarding that regime, Ref. [12] compared various parametrizations of f_{xc} alone against the QMC data and remarked about supposedly

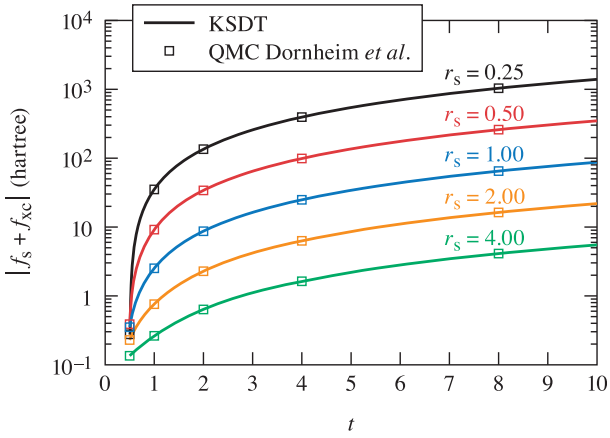

FIG. 2. Comparison between the total free energy per particle from the KSDT parametrization and data from Ref. [2] for the unpolarized HEG at $r_s = 4, 2, 1, 0.5$ (calculated by using data from the last column in Table II in the Supplemental Material), and at $r_s = 0.25$ data from the GDB fit [6].

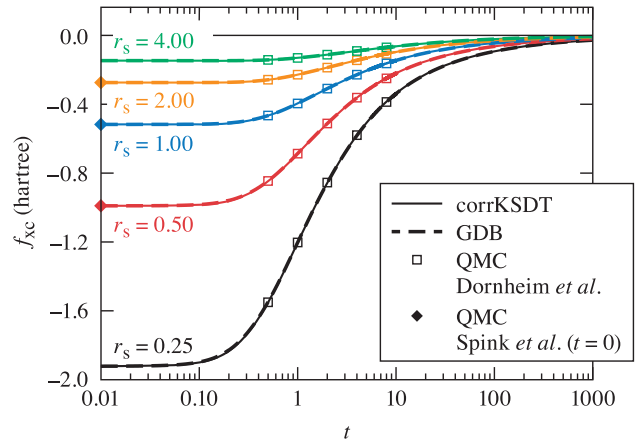

FIG. 3. Comparison between f_{xc} values from the corrKSDT and GDB parametrizations and QMC data from Ref. [13] for the unpolarized HEG at $r_s = 0.25, 0.5, 1, 2$ and 4. The ground-state limit ($t = 0$, Ref. [5]) QMC values also are shown.

significant errors in $\Delta f_{xc}/f_{xc}$ at $r_s = 1$, $t = 8$ and $r_s = 0.1$, $t = 4$. But the relevant point is that the relative *total* free-energy error $\Delta f_{tot}/|f_{tot}|$ at those points is 0.017% and 0.0045%, respectively. See the Supplemental Material of Ref. [8] for detail. Figure 1 shows that, in this high-density regime and especially if temperature is high, the XC term is a few orders of magnitude smaller as compared with the upper bound of the total free energy, therefore the exchange-correlation does not play any role.

Since the HEG *per se* is the system of interest, one must compare corrKSDT and GDB for f_{xc} alone (recall that the noninteracting contribution is known exactly in this case). A successful representation requires two ingredients, QMC data accurate over the (r_s, t) plane and an analytical fitting procedure constrained by existing theories, thermodynamic consistency, and exact limits. References [5] and [2] provided accurate QMC data for the HEG over a wide density range at $t = 0$ and $0.5 \leqslant t \leqslant 8$, respectively. The required sophisticated fitting procedure was developed in Ref. [4]. The two most accurate fits to the HEG XC free energy, corrKSDT [8], and GDB [6], both use that analytical fitting procedure and QMC data sets.

In the case of GDB, the lack of low-t QMC data ($t < 0.5$) was addressed by approximate theoretical STLS results [7]. For the same purpose, in the present work we used the original KSDT fit to generate data for $t < 0.5$ (those data are accurate for this temperature range as confirmed in Refs. [2] and [13]) to complement the QMC data (at $t \geqslant 0.5$) for the corrKSDT parametrization.

As an aside, the reasons for KSDT accuracy in that regime deserve comment. The key point is that the KSDT representation is not simply a fit to the Ref. [1] QMC data. Rather, the KSDT parametrization also was constrained by existing theories, thermodynamic consistency, and exact limits. Deficiencies in the QMC data or finite-size corrections therefore did not necessarily propagate directly to KSDT. This is confirmed by a result from Ref. [13]. Those authors showed that the Brown *et al.* QMC data [1] are somewhat inaccurate at $r_s = 1.0$, 0.1, and 0.25. To the resolution shown in Fig. 5 of Ref. [13], the KSDT parametrization does not reproduce the incorrect Brown *et al.* data for $r_s = 1.0$ but instead matches the subsequent data of Ref. [13] almost perfectly. This is a consequence of the KSDT construction, as confirmed by the fact that the same figure in Ref. [13] shows that KSDT results lie very close to the second-order analytical results known as the "e^4" approximation [14].

The outcome is that, despite some differences in low-t treatment, the two fits, corrKSDT and GDB, become practically identical. The mean absolute relative deviation for f_{xc} calculated over the 72 (r_s, t)-data points used for the corrKSDT representation is only 0.1%. The maximum relative deviation is 0.3% (see details in Supplemental Material of Ref. [8]). Figure 3 demonstrates that the two fits match the available QMC data indistinguishably for $t \geqslant 0.5$ and are in virtually perfect agreement for $t < 0.5$.

III. THERMODYNAMIC DERIVATIVES

A. Unpolarized homogeneous electron gas

The total free energy is the state function whose derivatives with respect to density and temperature provide other thermodynamic quantities of interest. Consider first the entropy per particle, $\sigma(r_s, t)$:

$$\sigma(r_s, t) = -\frac{1}{T_F} \frac{\partial f(r_s, t)}{\partial t}\bigg|_{r_s}. \tag{3}$$

Burke *et al.* [15] found that the KSDT representation for $f(r_s, t)$ leads to a HEG total entropy per particle that goes negative over a remote region of state space, roughly $r_s \geqslant 10$ and $t \leqslant 0.1$. Immediately, the negligible impact of that anomaly for WDM calculations was confirmed [16], although it is a flaw in the KSDT representation. As part of the corrKSDT reparametrization (to correct the $T = 0$ data error in KSDT), entropy positivity was enforced up through $r_s = 75$. This is between the first HEG phase transition (polarized liquid) and Wigner crystallization [17]. The rationale is that those phase boundaries should delineate the limiting range of the fit

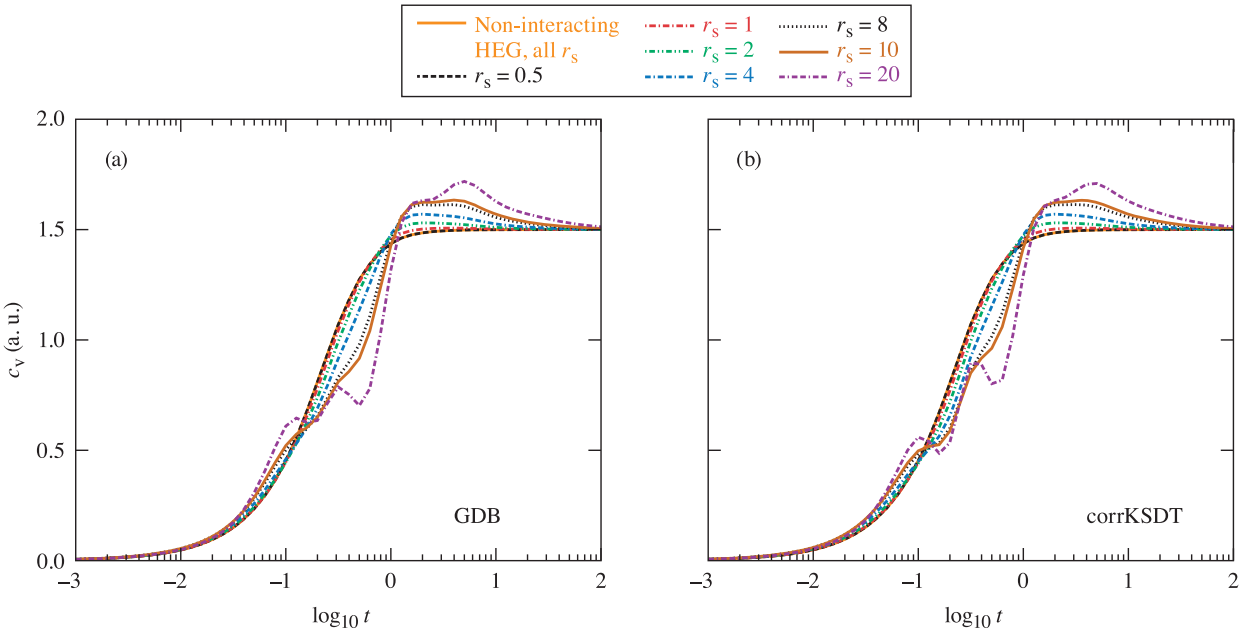

FIG. 4. Electron specific heat c_V for the noninteracting and interacting HEG calculated with (a) GDB and (b) corrKSDT parametrizations.

(see further discussion below). The perhaps expectable result (given the equivalence of the two parametrizations) is that negative entropies still are obtained by using the corrKSDT and GDB representations, but the onset of negative entropy is at very high r_s values (near 80 and higher). In summary, there is no fundamental concern about these representations for the entropy per particle so long as HEG phase transitions are not an issue.

Next, consider the electron specific heat, $c_V(r_s, t)$:

$$c_V(r_s,t) = -\frac{t}{T_F}\frac{\partial^2 f(r_s,t)}{\partial t^2}\Big|_{r_s} = \frac{1}{T_F}\frac{\partial \varepsilon(r_s,t)}{\partial t}\Big|_{r_s}. \quad (4)$$

It is well known that small errors in a fitted function may produce large errors in high-order derivatives. The specific heat thus is a challenging property because of its dependence upon the second temperature derivative of $f(r_s, t)$ or upon the first derivative of the internal energy $\varepsilon(r_s, t) = \tau_s(r_s, t) + \varepsilon_{xc}(r_s, t)$ represented as a sum of the noninteracting kinetic and XC internal energy terms. Figure 4 shows c_V calculated for the noninteracting and interacting HEG from the corrKSDT and GDB representations. As anticipated, the specific heat curves from the two parametrizations are practically identical, a consequence of the small procedural differences of parameter fitting in the two. However, in both cases an unexpected oscillatory behavior for t between 0.1 and 1 for $r_s \geqslant 10$ is seen, increasing in amplitude with increasing r_s. Although that oscillatory behavior might be an indication of some kind of critical point, it is far more plausible that it is an artifact introduced by the QMC data of Ref. [2] and the way that corrKSDT and GDB represent those data.

Pursuing that point, further analysis shows that the representations for the X and C contributions to the internal energy, ε_x and ε_c, have opposite slopes for t between 0.1 and 4 and both slopes change sign at $t \approx 0.2$ [see $r_s = 10$ curve in Fig. 5(a)]. A small dip on the ε_x curve and a bump on the ε_c curve produce oscillations in the $d\varepsilon_x/dt$ and $d\varepsilon_c/dt$ derivatives. For c_V the oscillations are amplified by a $1/T_F$ prefactor which is large for large r_s. The two lower panels in Fig. 5 show the X and C contributions to the internal energy derivative. Observe that there are significant cancellations between those contributions. The cancellation is almost total for $r_s \geqslant 10$. That leads to a drastic decrease of accuracy for c_V. A small

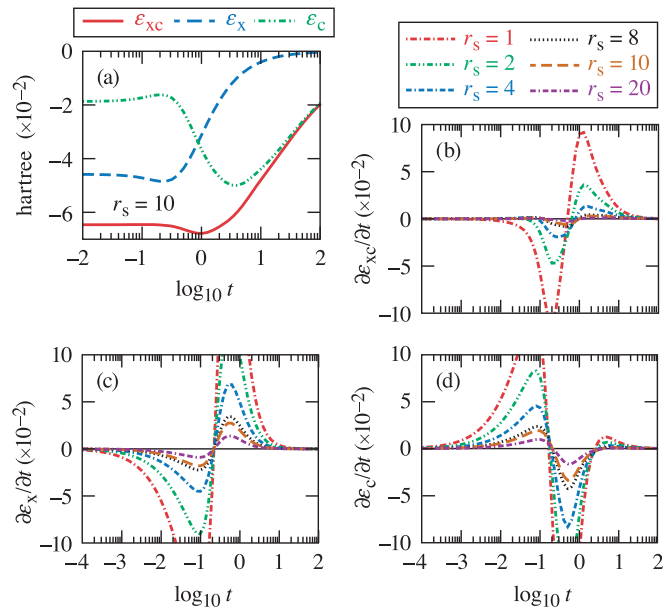

FIG. 5. Upper panels: (a) ε_{xc}, ε_x and ε_c energy per particle as a function of temperature for $r_s = 10$ and (b) $d\varepsilon_{xc}/dt$ derivative. Lower panels: (c) $d\varepsilon_x/dt$ and (d) $d\varepsilon_c/dt$ derivatives. All quantities calculated with GDB; corrKSDT gives virtually identical results.

relative error in the $d\varepsilon_c/dt$ derivative may, after cancellation between the large-magnitude X and C contributions followed by multiplication by the large prefactor $1/T_F$, yield a large error in c_V. Denser QMC sampling in r_s at large r_s and low t should improve the fit accuracy (there is nothing else available to constrain or shape the fit for $r_s > 10$) and reduce errors in temperature derivatives.

Whether the cancellation-induced oscillations in c_V would occur in LDA calculations on realistic physical systems is an open question that at this point is obscured by computational technique. In the usual technique, c_V is obtained from differentiating a convenient analytical representation of the total internal energy. That analytical expression is fit to internal energy calculations at various T for a fixed volume V. The approach is motivated by the fact that separate analytical temperature derivatives of the exchange and correlation free energies are not implemented in any code of which we are aware. In ordinary calculations there simply is no interest in those individual contributions. Expenditure of effort on such implementation therefore is unlikely to be a priority until an explicit focus of research is to resolve the peculiar c_V behavior that we have identified here in the HEG. That is substantially beyond the scope of the present work.

One aspect of the foregoing analysis deserves mention; namely, the partitioning into X and C contributions. For $f_{xc} = f_x + f_c$, we have

$$f_x(r_s,t) = -\frac{1}{2\pi^3\beta^2}\int_{-\infty}^{\eta}\left[I_{-1/2}(\eta)\right]^2 d\eta \equiv \widetilde{A}_x(t)e_x(r_s),$$
$$f_c(r_s,t) = f_{xc}(r_s,t) - f_x(r_s,t). \tag{5}$$

Here $\eta := \beta\mu$, $\beta := (k_B T)^{-1}$, I_α is the Fermi–Dirac integral, μ is the chemical potential defined by the average density n, $e_x = -\frac{3}{4}(\frac{3}{\pi})^{1/3}n^{1/3}$ is the zero-T LDA X energy per particle, and $\widetilde{A}_x$ is given by the very accurate analytical fit given by Eq. (39) in Ref. [18]. Internal XC, X, and C energy contributions are calculated with use of Eq. (5) and the standard thermodynamic relation

$$\varepsilon_{x/c}(r_s,t) = f_{x/c}(r_s,t) - t\left.\frac{\partial f_{x/c}(r_s,t)}{\partial t}\right|_{r_s}. \tag{6}$$

The point of the preceding summary is that the XC decomposition used here is *not* the same as the implicit decomposition used to construct corrKSDT, KSDT, and GDB. In them, the first function in the numerator of the KSDT Padé approximant [called $a(t)$, Eq. (10) in Ref. [4]] in t is, in fact, the Perrot–Dharma-wardana approximation for f_x [19,20]. Crucially, however, we never use that $a(t)$ to extract f_x. Rather, $a(t)$ appears in KSDT (hence also in corrKSDT and GDB) only as a reasonably good f_x approximation which then is corrected by the other functions and fitting parameters in the remainder of the KSDT form for the combined X and C representation f_{xc}. As a result, only in the high-density (low-r_s) limit does $f_{xc} \to f_x \approx a(t)$, which is the Perrot–Dharma-wardana exchange.

In constructing the KSDT representation, four formally equivalent thermodynamic routes (Maxwell relations) were tested, after which the so-called route A was selected; see Ref. [4] for details. corrKSDT in contrast used route B which is based on use of the QMC potential-energy data only. GDB also had to use route B (see Ref. [3], section 8.2.5). As already noted, the two yield very similar HEG c_V behavior. We suspect that the use of routes C or D might give different c_V results for large r_s than the values obtained from using route A or B. We do not, however, have all the QMC data (and finite-size corrections) required to use routes C and D to obtain alternative parametrizations to corrKSDT and test this speculation.

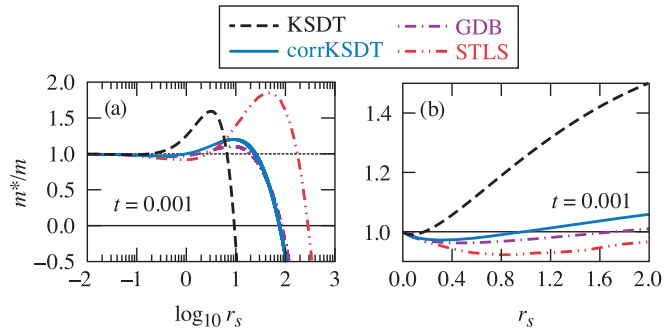

FIG. 6. Effective-mass enhancement calculated from the KSDT, corrKSDT, GDB, and STLS (taken from Ref. [22]) parametrizations at $t = 0.001$. Overview left, expanded view right.

The limiting behavior of the electron specific heat at low T defines the Fermi-liquid effective mass m^*:

$$\frac{m^*}{m} = \lim_{t\to 0}\frac{c_V(r_s,t)}{c_{V,s}(t)}, \tag{7}$$

where $c_{V,s}(t)$ is the noninteracting system specific heat. For corrKSDT, KSDT, and hence for GDB, the small-t series expansion of the XC internal energy ε_{xc} by construction has quadratic and higher-order terms but no linear-t term. Therefore the specific heat exhibits physically correct linear low-t behavior [21], $c_V \sim t$.

On fundamental grounds, both $c_V(r_s,t)$ and $c_{V,s}(t)$ are linear in t for small t, so the effective mass should approach a limit dependent only on r_s. The functional representations of corrKSDT and GDB therefore preserve this behavior, despite the fact that they are not based on any data below $t < 0.0625$.

A recently discovered oddity [22] is that m^*/m obtained from the KSDT representation has a larger amplitude variation on $0 \leqslant r_s \leqslant 1$ than generally has been expected [23]. Prior calculations have that amplitude range as roughly $0.95 \leqslant m^*/m < 1$ whereas KSDT gives about $0.98 \leqslant m^*/m \leqslant 1.2$. The prior calculations involve assumptions and techniques the consequences of which are difficult to assess. Hence it is not clear that the KSDT result is wrong, only that it is unexpected. Since no QMC data were or are available for $t < 0.0625$ and $r_s \leqslant 1$, KSDT was forced to be an extrapolation to the $T = 0$ data of Ref. [5] as well as an extrapolation from $r_s = 1$ downward. The more recent QMC data [2] do not resolve that issue, as they are limited to $t \geqslant 0.5$. The unusual enhancement, m^*/m, occurs as well for the improved representations corrKSDT and GDB, as shown in Fig. 6.

B. Spin-polarization anomaly

All of the discussion above refers to the unpolarized HEG. More generally, however, the representations depend on the

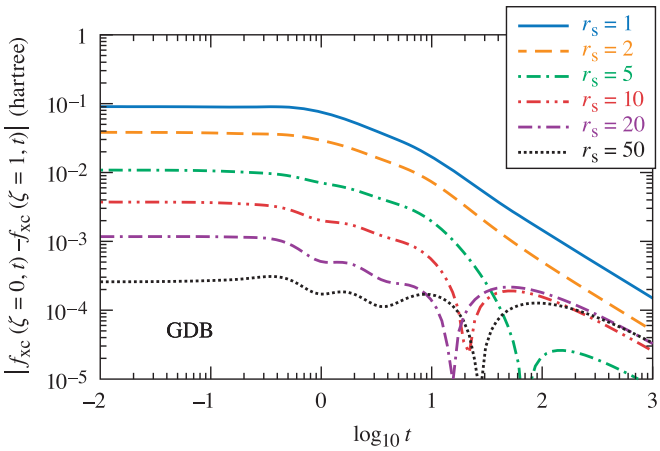

FIG. 7. $|\Delta f_{\mathrm{xc,pol}}|$ Eq. (8) from GDB.

degree of polarization. The difference in fully spin-polarized and -unpolarized XC free energies,

$$\Delta f_{\mathrm{xc,pol}}(r_s, t) := f_{\mathrm{xc};\zeta=0}(r_s, t) - f_{\mathrm{xc},\zeta=1}(r_s, t), \qquad (8)$$

is related to the spin stiffness. At $T = 0$ it is defined as $\partial^2 \epsilon_{\mathrm{xc}}/\partial \zeta^2|_{\zeta=0}$ [24,25]. Values of $|\Delta f_{\mathrm{xc,pol}}|$ calculated from GDB are plotted in Fig. 7 as a function of t. One sees that the high-temperature behavior is very different for $r_s = 1, 2$ and $r_s \geqslant 5$ (remark: data between $r_s = 2$ and 5 were not checked): $\Delta f_{\mathrm{xc,pol}}$ for $r_s = 1, 2$ is positive for all values of t, but this difference develops a sign change at larger r_s values. For example, $\Delta f_{\mathrm{xc,pol}}$ becomes negative at $t \approx 70$ and $t \approx 20$ for $r_s = 5$ and 10, respectively. The equivalence of corrKSDT and GDB representations once again is relevant. Recall that the parametrization of corrKSDT was constrained explicitly to avoid negative entropies through the HEG zero-temperature spin-polarization transition $r_s \approx 70$ (Ref. [17]) but below the Wigner crystal transition. The rationale for the latter choice is that extrapolation by a continuous function in r_s across a symmetry-breaking phase transition is indefensible. The former choice is rationalized by the notion that the zero-temperature spin polarization r_s is far above the largest value for which finite-T QMC data are available, so the zero-T polarization r_s is best used to provide a limit on the range of constraint enforcement (e.g., entropy positivity) and not as a constraint in and of itself. This logic applies for GDB as well. Therefore, it is questionable as to whether the GDB sign changes $\Delta f_{\mathrm{xc,pol}}$ are meaningful. Also, perceptible oscillations develop for large r_s that do not seem physical [26]. While the oscillations are large percentage-wise, they are with respect to a very small magnitude. Absent any knowledge of error bars on $\Delta f_{\mathrm{xc,pol}}$ therefore, the oscillations seem largely immaterial: it makes little difference whether the value at $r_s = 50$ is 0.0002 or 0.0003. Note again that $r_s = 50$ is outside the range of state conditions for which there was parametrization data.

The consistent theme thus uncovered is that a parametrization for f_{xc} which provides accurate high-order temperature derivatives will require very accurate QMC data for $t < 0.5$ and appropriate sampling of the large-r_s region.

IV. DATA ACCURACY VERSUS FITTING ACCURACY

In the main, the accuracy of an f_{xc} fit relies on the accuracy of the reference QMC data and the extent to which exact constraints, limits, and thermodynamic consistency are implemented in the underlying fitting procedure. The other accuracy issue to be taken into account is error introduced by the fitting procedure itself. Procedures used in Ref. [2] provide a way to assess that. Those authors used one of the thermodynamic routes defined in Ref. [4] to obtain $f_{\mathrm{xc}}^{\mathrm{fit}}$ from their accurate reference QMC potential-energy data V^{QMC} (combined with the STLS data at $t < 0.5$): $V^{\mathrm{QMC}} \rightarrow f_{\mathrm{xc}}^{\mathrm{fit}}$. To estimate the accuracy of that fit, we used a thermodynamic consistency test from Ref. [4]; namely, regeneration of the potential energy from the fitted XC free energy: $f_{\mathrm{xc}}^{\mathrm{fit}} \rightarrow V^{\mathrm{fit}}$. Comparison between the original QMC values V^{QMC} and data obtained from the fit, V^{fit}, gives an error estimate for $f_{\mathrm{xc}}^{\mathrm{fit}}$, as

$$\Delta f_{\mathrm{xc}}^{\mathrm{fit}} \approx \Delta V = (V^{\mathrm{QMC}} - V^{\mathrm{fit}}). \qquad (9)$$

We obtain $\Delta V = -0.0011$ Hartree for $t = 0.5$ and $r_s = 4$, and relative errors, $\Delta f_{\mathrm{xc}}^{\mathrm{fit}}/|f_{\mathrm{xc}}^{\mathrm{fit}}| = 0.7\%$, $\Delta V/|V^{\mathrm{QMC}}| = 0.8\%$. Both are significantly larger than the relative error of 0.1% for the QMC V data reported in Ref. [2].

We note that Ref. [2] did something different from the KSDT protocols that were used to determine GDB. Instead, they used a set of fixed-temperature fits of smooth r_s-dependent functions, not a fit of a two-variable function to the entire set of accurate QMC data. Error control in such fixed-t fits is easier than for the two variables because the r_s- dependence of f_{xc} at fixed t is rather featureless compared with its t dependence at fixed r_s. A challenge to full two-variable parametrization therefore is to avoid introducing much larger fitting errors than those in the underlying QMC data when a full r_s, t representation is built.

V. EXCHANGE-CORRELATION APPROXIMATIONS

In the context of free-energy DFT, inhomogeneous systems and not the HEG *per se* are the focus. What then is critical is whether the analytical representation errors for corrKSDT and GDB are acceptable, on the energy scale of their intended application, for using those representations as the LDA for DFT.

There are two types of applications. One is as the f_{xc} approximation itself. The other is as a key ingredient in more sophisticated XC approximations. Long experience with applications of ground-state DFT confirms that such more advanced XC approximations (than the LDA) are required to get the physics of many systems right. The first step of refinement beyond the LDA is to incorporate density-gradient dependence in the form of GGAs [27]. They utilize a gradient-driven local modulation of the LDA, so a very-high-quality LDA is an essential ingredient. A highly pertinent example is our recently presented KDT16 XC free-energy approximation for finite T [8]. The first nonempirical GGA f_{xc}, it has the corrKSDT representation as a key ingredient.

Systematic address of the issue of the legitimacy of an f_{xc} HEG representation as an LDA is helped by delineation of the WDM regime. (By construction, the $T = 0$ behavior of corrKSDT, KSDT, and GDB is guaranteed to be the correct

LDA.) The low-density end of the WDM density regime, hence the largest relevant r_s value, is arguably about 10. H; for example, at bulk density, $\rho_H = 0.005$ g/cm^3 is about a factor of 17 below the liquid H density, yet has $r_s = 8.1$. Similarly $r_s = 7.8$ for aluminum at $\rho_{Al} = 0.05$ g/cm^3. That is a factor of 50 smaller than ambient bulk solid Al density. Conversely, even rather modest r_s values correspond to extraordinarily highly compressed systems. As an example $r_s = 0.25$ corresponds to roughly 2000-fold compressed hydrogen ($\rho_H = 180$ g/cm^3). For $0.25 \leqslant r_s \leqslant 10$ the relevant reduced temperature range, $0.5\text{eV} \leqslant k_B T \leqslant 10$ eV is roughly $0 \leqslant t \leqslant 20$. Figure 1 shows that a significant part of these physically relevant ranges ($r_s \gtrsim 4$, $t < 0.5$) belongs to the critical density-temperature region wherein no accurate reference QMC data for the HEG are available to date.

The pertinent point is that those ranges are either within the ranges discussed already with respect to HEG representation fidelity or are verging on high-t limits. Thus $\Delta f_{tot}/|f_{tot}|$, Eq. (2), for corrKSDT never exceeds about 0.02% for the HEG and the most conservative estimate of error [8] is 0.3% up to $t = 10$. Matters improve as t grows beyond that. This focus on f_{tot} errors is critical, because focus on f_{xc} errors can be quite misleading. The decomposition, Eq. (1), is important primarily to isolate the quantity for which approximation is required and as a route to computational feasibility (e.g., the Kohn–Sham procedure). That decomposition is *unimportant* for many physical quantities of interest (e.g., pressure).

To be specific, in the WDM regime, DFT calculations of quantities for which the effects of explicit T dependence in the XC free energy are significant include the equation of state (EOS), thermal properties, and optical and direct current (dc) conductivity [16]. The first two of those exemplify quantities for which the decomposition is only an instrumentality, a route to the dependence upon f_{tot}. The third type of quantity (transport coefficients), at least as calculated in the Kubo–Greenwood approximation [28], does depend on the details of the decomposition (2) through sums of quantities (e.g., matrix elements) dependent upon the Kohn–Sham orbitals and eigenvalues. The values of such sums, however, depend only weakly upon small detailed differences in LDA versions.

As an aside, Ref. [12] includes speculation as to possible inaccuracy in the KSDT spin interpolation function. The question is whether this matters for DFT application. That seems doubtful. KSDT spin-interpolation faithfully recovers the Spink *et al.* [5] ground-state partially polarized QMC results. There seems little reason, therefore, to expect meaningful improvement from matching to partially polarized finite-T QMC results, although it would be interesting to have them if only for confirmation.

The foregoing facts and reasoning confirm that all three HEG representations for $f(r_s, t)$, corrKSDT, KSDT, and GDB are essentially equivalent as satisfactory f_{xc} LDAs.

VI. SUMMARY

Three objectives have been achieved. The first is based on recent simulation studies of the free energy for the HEG in a domain of the (r_s, t) plane not previously explored. The data combined with thermodynamic consistency and known theoretical limits led to three global representations of the free energy, corrKSDT, its direct antecedent KSDT, and GDB. In Sec. II the equivalence of these for reproducing the simulation data for $f(r_s, t)$ was demonstrated. Furthermore, the equivalence of corrKSDT and GDB for the XC component alone was illustrated, although the original KSDT representation has some small, inconsequential errors for $f_{xc}(r_s, t)$ [2].

The second objective was to draw attention to the fact that, in spite of these very accurate representations for $f(r_s, t)$, derived thermodynamic properties obtained by temperature derivatives exhibit suspicious anomalies. Those occur outside the domain for which simulation data are available and are properties of the extrapolation or interpolation provided by the fitting procedure. This was discussed in Sec. III where it was noted that the entropy per particle (first-order temperature derivative) can become negative for large r_s and small t. For the corrKSDT and GDB representations, this corresponds to state conditions beyond the expected spin-polarization transition and therefore outside the domain of their intended application. A second, more serious anomaly occurs for the specific heat (second derivative with respect to T). In that case, all three representations predict unusual oscillatory behavior for t between 0.1 and 1 and $r_s \geqslant 10$. Without any theoretical or simulation guidance, this must be seen as a possible flaw in the representation function. A related question is the enhanced Fermi liquid relative effective mass (defined as the ratio of the interacting and noninteracting specific heat at $T = 0$). Calculations based on the three representations and the STLS theoretical model are shown in Fig. 6. Those results differ from expectations from approximate (uncontrolled) Fermi-liquid theories. In the present context it must be considered that this difference may be due to the form of the fitting function. Finally, Sec. III B considered the polarization dependence of the exchange free energy; specifically, the difference between the unpolarized and polarized results $\Delta f_{xc,pol}(r_s, t) := f_{xc;\zeta=0}(r_s, t) - f_{xc,\zeta=1}(r_s, t)$. The results calculated from the GDB representation are shown in Fig. 7. The oscillations at low t increasing in amplitude with increasing r_s are unexplained and potentially unphysical.

The third objective was to verify the use of the three representations as essential interchangeable for use as LDA functionals in free energy DFT calculations and in more refined f_{xc} approximations. It is helpful to note the parallel with most $T = 0$ DFT calculations. They are based in a similar way on ground-state HEG simulations. Generalized gradient approximations, for example, have the LDA (hence the HEG) as a limiting case. Therefore, the extensions discussed here to the entire (r_s, t) plane constitute an essential prerequisite for addressing WDM in an accurate, practical fashion. A first example of a nonempirical semilocal free-energy density functional for matter under extreme conditions, built on the LDA representations here was noted [8].

As for the advocacy for a more accurate fit to f_{xc} in Refs. [2] and [6], the arguments given here suggest those calls to have been ill-timed. The demonstrated indistinguishability of corrKSDT and GDB stands as confirmation. Going forward, there is an essential prerequisite to achieving a representation that represents HEG thermodynamics substantially better. That prerequisite is *new adequately accurate and densely spaced QMC data to resolve the anomalies that we have discussed.* Without such data, an allegedly

better fit would be premature, if not outright misleading. While the anomalies we have highlighted are of no direct importance for DFT calculations of WDM, they are important signatures of physical effects that must be addressed for a better understanding of the HEG. A very high quality representation of the HEG free energy would provide an unassailable benchmark against which to test ingenious but uncontrolled many-body approximation methods and simulation methods.

ACKNOWLEDGMENTS

We thank F. Eich, T. Rejec, and G. Vignale for communication of their results prior to publication.

This material is based upon work supported in part by the Department of Energy National Nuclear Security Administration under Award Number DE-NA0003856, US National Science Foundation PHY Grant No. 1802964, the University of Rochester, and the New York State Energy Research and Development Authority. JWD and SBT acknowledge support by U.S. Department of Energy Grant DE-SC 0002139.

[1] E. W. Brown, B. K. Clark, J. L. DuBois, and D. M. Ceperley, Phys. Rev. Lett. **110**, 146405 (2013).
[2] T. Dornheim, S. Groth, T. Sjostrom, F. D. Malone, W. M. C. Foulkes, and M. Bonitz, Phys. Rev. Lett. **117**, 156403 (2016).
[3] T. Dornheim, S. Groth, and M. Bonitz, Phys. Rep. **744**, 1 (2018).
[4] V. V. Karasiev, T. Sjostrom, J. W. Dufty, and S. B. Trickey, Phys. Rev. Lett. **112**, 076403 (2014).
[5] G. G. Spink, R. J. Needs, and N. D. Drummond, Phys. Rev. B **88**, 085121 (2013).
[6] S. Groth, T. Dornheim, T. Sjostrom, F. D. Malone, W. M. C. Foulkes, and M. Bonitz, Phys. Rev. Lett. **119**, 135001 (2017).
[7] S. Tanaka and S. Ichimaru, J. Phys. Soc. Jpn. **55**, 2278 (1986).
[8] V. V. Karasiev, J. W. Dufty, and S. B. Trickey, Phys. Rev. Lett. **120**, 076401 (2018).
[9] T. Dornheim, S. Groth, F. D. Malone, T. Schoof, T. Sjostrom, W. M. C. Foulkes, and M. Bonitz, Phys. Plasmas **24**, 056303 (2017).
[10] D. M. Ceperley, Rev. Mod. Phys. **67**, 279 (1995).
[11] F. D. Malone, N. S. Blunt, J. J. Shepherd, D. K. K. Lee, J. S. Spencer, and W. M. C. Foulkes, J. Chem. Phys. **143**, 044116 (2015).
[12] S. Groth, T. Dornheim, and M. Bonitz, Contrib. Plasma Phys. **57**, 137 (2017).
[13] T. Schoof, S. Groth, J. Vorberger, and M. Bonitz, Phys. Rev. Lett. **115**, 130402 (2015).
[14] J. Vorberger, M. Schlanges, and W.-D. Kraeft, Phys. Rev. E **69**, 046407 (2004).
[15] K. Burke, J. C. Smith, P. E. Grabowski, and A. Pribram-Jones, Phys. Rev. B **93**, 195132 (2016).
[16] V. V. Karasiev, L. Calderín, and S. B. Trickey, Phys. Rev. E **93**, 063207 (2016).
[17] D. M. Ceperley and B. J. Alder, Phys. Rev. Lett. **45**, 566 (1980).
[18] V. V. Karasiev, D. Chakraborty, and S. B. Trickey, Comput. Phys. Commun. **192**, 114 (2015).
[19] F. Perrot and M. W. C. Dharma-wardana, Phys. Rev. A **30**, 2619 (1984); see particularly Eqs. (a31)–(a33).
[20] S. Ichimaru, Rev. Mod. Phys. **65**, 255 (1993).
[21] A. Tari, *The Specific Heat of Matter at Low Temperatures* (Imperial College Press, London, 2003).
[22] F. G. Eich, M. Holzmann, and G. Vignale, Phys. Rev. B **96**, 035132 (2017).
[23] G. F. Giuliani and G. Vignale, *Quantum Theory of the Electron Liquid* (Cambridge University Press, Cambridge, 2005), Sec. 8.8 and references therein.
[24] S. H. Vosko, L. Wilk, and M. Nusair, Can. J. Phys. **58**, 1200 (1980).
[25] J. P. Perdew and Y. Wang, Phys. Rev. B **45**, 13244 (1992).
[26] T. Rejec (private communication).
[27] J. P. Perdew and K. Schmidt, in *Density Functional Theory and its Applications to Materials*, edited by V. Van Doren, C. Van Alsenoy, and P. Geerlings, AIP Conf. Proc. No. 577 (AIP, New York, 2001), pp. 1.
[28] J. W. Dufty, J. Wrighton, K. Luo, and S. B. Trickey, Contrib. Plasma Phys. **58**, 150 (2018), and references therein.